Supporting information

Controlled Nanopore Sizes in Supraparticle Supports for Enhanced Propane Dehydrogenation with GaPt SCALMS Catalysts

Nnamdi Madubuko [a,‡], Umair Sultan [a,b,‡], Simon Carl [c], Daniel Lehmann [a], Xin Zhou [c], Alexander Soegaard [a], Nicola Taccardi [a], Benjamin Apeleo Zubiri [c], Susanne Wintzheimer [d], Erdmann Spiecker [c], Marco Haumann [a,e], Nicolas Vogel [b*], Peter Wasserscheid [a,f*]*

[a] Friedrich-Alexander-Universität Erlangen-Nürnberg (FAU), Lehrstuhl für Chemische Reaktionstechnik (CRT), 91058, Erlangen, Germany

[b] Friedrich-Alexander-Universität Erlangen-Nürnberg (FAU), Institute of Particle Technology, 91058, Erlangen, Germany

[c] Friedrich-Alexander-Universität Erlangen-Nürnberg (FAU), Institute of Micro- and Nanostructure Research (IMN) & Center for Nanoanalysis and Electron Microscopy (CENEM), IZNF, 91058 Erlangen, Germany

[d] Friedrich-Alexander-Universität Erlangen-Nürnberg (FAU), Department of Chemistry and Pharmacy, Inorganic Chemistry, 91058, Erlangen, Germany; Fraunhofer-Institute for Silicate Research ISC, Neunerplatz 2, 97082 Würzburg, Germany

[e] University of Johannesburg, Department of Chemistry, Research Centre for Synthesis and Catalysis, P.O. Box 524, Auckland Park 2006, South Africa

[f] Forschungszentrum Jülich GmbH, Helmholtz-Institute Erlangen-Nürnberg for Renewable Energy (IEK-11), 91058, Erlangen, Germany; Forschungszentrum Jülich GmbH, Institute for a Sustainable Hydrogen Economy (INW), 52428 Jülich, Germany

E-mail address: peter.wasserscheid@fau.de, marco.haumann@fau.de, nicolas.vogel@fau.de

Methods

Materials

All chemicals were used as received. Gallium nuggets (size 3 mm, purity: 99.999%, Alpha Aesar), hexachloroplatinic acid (Pt bases: ≥ 37.5%, Sigma-Aldrich), propan-2-ol (purity ≥ 99.8%, VWR chemicals). absolute ethanol (≥99.8%, NORMAPUR®, VWR), ammonium hydroxide (25%, NORMAPUR®, VWR), tetraethyl-orthosilicate (TEOS, ≥99 %, GPR RECTAPUR®, VWR), hydrochloric acid (HCl, 37%, VWR), acrylic acid (99 %, Sigma Aldrich), ammonium persulfate (≥98.0%, Sigma Aldrich), sodium hydroxide (NaOH, ≥98 %, Ph. Eur., USP, BP, in pellets), aluminum oxide (90, neutral). Styrene (ReagentPlus®) was washed with 10 wt% aqueous NaOH solution and then passed through an aluminium oxide column to remove inhibitor. It was then stored no longer than 2 months at 8 °C before use. For water, a Purelab Flex 2 (Elga Veolia) purification unit was used (18.2 MΩ cm).

Synthesis of GaPt-SCALMS catalyst

The GaPt SCALMS catalyst was prepared using two main steps as described using Figure 2. In the first step, the gallium nanoparticle dispersion (GaNP-dispersion) was prepared via ultrasonication (Branson sonifier SFX 550 equipped with a microtip). Prior to the ultrasonication, the desired amount of Ga was pre-melted in an oven at 80 °C for 30 min. The pre-melting ensures the liquid state of gallium directly from the start of the sonication.[1] Once melted, gallium can remain in a supercooled liquid state at temperatures below the melting point for days. After pre-melting step, the ultrasonication of Ga nuggets were performed in 100 mL of propa-2ol using 72 % of sonifier power for 30 min at a maximum temperature of 50 °C. The formed Ga dispersion by ultrasonication leads to a broad particle size distribution up to 1 µm as reported in our previous work.[2,3] To obtain Ga NP < 300nm for impregnation in supports with large pores up to 400 nm, a centrifugation step was introduced. The entire Ga dispersion was centrifuged at 1200 rpm (225 rcf) for 10 min in a HERMLE Labortechnik centrifuge Z 366. The supernatant obtained after centrifugation contained Ga droplets < 300 nm. This was confirmed by DLS and SEM image analysis. The residue was recycled to increase yield of the desired size fraction as shown in Figure S1.

Support impregnation and galvanic displacement

In the second step, the prepared Ga-dispersion with particle sizes < 300 nm was physically deposited on the respective support by wet impregnation. The amount of the Ga-dispersion and the support used was regulated to achieve a 6 wt% loading of Ga on the support. After 5 min of stirring, the solvent was slowly removed using a rotary evaporator at 313 K, 0.0078 MPa and calcined under air at 773 K for 3 h. Based on the Ga loading on the decorated support determined by ICP-AES, the catalytically active metal, Pt was introduced by galvanic displacement reaction (Eq. 1) using a hexachloroplatinic acid precursor ($H_2PtCl_6 \,.\, 6H_2O$) with Pt concentration of $C_{precusor} = 4.4\, mg_{Pt}\, mL^{-1}$. The amount of Pt introduced was calculated using Eq 2.

$$4Ga^o + 3Pt^{4+} \rightarrow 4Ga^{3+} + 3Pt^o \quad (1)$$

$$m_{Pt} = \frac{\frac{w_{Ga}.m_{support}}{MW_{Ga}}}{Ga/Pt}.MW_{Pt} \quad (2)$$

The Ga/Pt molar ratio targeted was 45. This molar ratio typically describes a GaPt alloy with 2.2 atom % of Pt in Ga. From the phase diagram, this represents a GaPt alloy that is liquid under typical alkane dehydrogenation reaction conditions of 773 K.[4] The final Ga and Pt loading of

all the catalyst prepared and tested in this work is summarized in Table S1. After 5 min of stirring, the solvent was slowly removed via a rotary evaporator at 313 K and then calcined under air at 773 K for 3 h. The metal Pt loading of the final catalyst was analysed by ICP-AES.

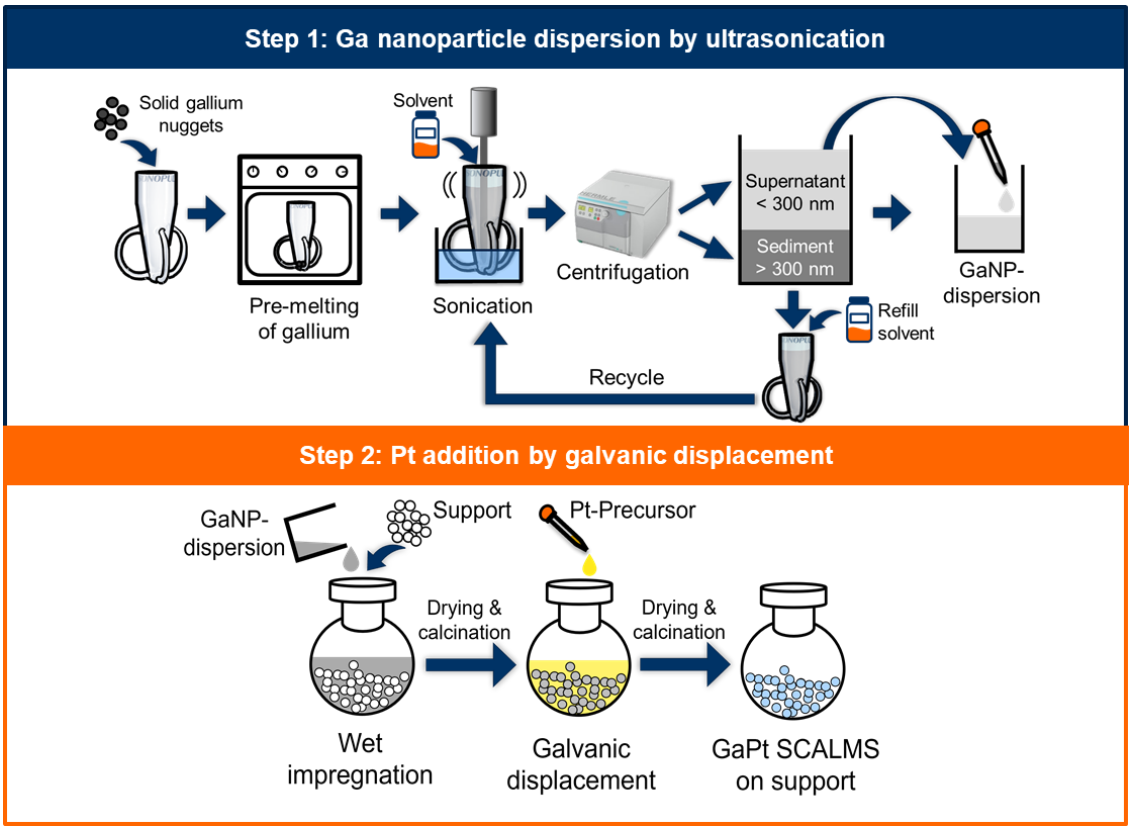

Figure S1. Preparation of GaPt SCALMS catalysts using two main steps. Step 1: formation of Ga nanopaticle dispersion with particle sizes < 300 nm by ultrasonication and centrifugation, step 2: deposition of Ga dispersion on catalyst support and addition of catalytic active metal, Pt by galvanic displacement

Synthesis of silica primary particles

Colloidal silica primary particles were synthesized via the Stöber method according to a modified procedure described in the literature.[5] In a typical reaction, water, absolute ethanol and NH_3 were mixed in a two liter, three-neck round bottom flask and continuously stirred at 300 rpm. TEOS was then added, and the solution was allowed to stir for 16 h at room temperature. The clear solution turned white overnight. These particles were separated from the synthesis solution via centrifugation, followed by cleaning with a mixture of water and ethanol 4 times. Afterwards, the particles were dispersed in water at a solid concentration of 50 wt%. The total volume of the synthesis solution was 1.6 L. The concentration of the ethanolic

synthesis solution was: 8 M water, 0.15 – 2 M NH_3, 0.3 M TEOS. The particle size was varied by changing the concentration of NH_3 from 0.15 M for 140 nm to 2 M for 650 nm.

Synthesis of polystyrene primary particles

Monodisperse polystyrene particles were synthesized via surfactant free emulsion polymerization, as reported in the literature.[6] 990 ml of water was heated to 76 °C inside a two liter three-necked round bottom flask using a heat block. During the heating time and during the reaction, the system was constantly flushed with nitrogen. A cooler provided reflux of condensate. After 2 h, styrene was added. In 10 min intervals, 0.4 g of acrylic acid and 0.4 g of ammonium persulfate, both dissolved in 5 ml of water, were added. After 22 h the nitrogen flow and heating were stopped, and the colloid was left to cool. To separate any coarse fractions, the colloid was filtered through a KIM Wipe (Kimberly-Clark). The particles were then recovered via centrifugation and washed 1 time with water-ethanol mixture and 3 times with water to remove any residual precursors. Then, they were dispersed in water at a solid concentration of 30 wt%. The particle size was adjusted by varying the styrene amount from 25- 50 g and varying stirring conditions.

Fabrication of Supraparticles

All supraparticle (SP) samples were produced by spray drying pure colloids and colloid mixtures with a spray-dryer (B290 Mini, BÜCHI Labortechnik) under nitrogen atmosphere. The colloid feed was atomized using a co-current flow two-fluid nozzle (Ø = 1.4 mm), at a gas flow of 357 L h^{-1} and feed flow of 3 mL min^{-1}. The aspirator flow was kept at 35 m^3 h^{-1} and the inlet temperature was set to 130 °C. The prepared SPs were fractionated using sieves of mesh sizes 63 µm and 300 µm to separate larger SPs for catalytic testing.

Characterization of surface morphology and particle size

SPs were imaged in SEM (Gemini 500, Zeiss) with an SE2 detector, at an acceleration voltage of 1 kV and aperture size of 15 µm. The working distance was kept at 6 mm. The particle sizes were measured via ImageJ software from multiple SEM images measured at higher magnifications and were subsequently converted to droplet volume distributions.

Characterization of textural properties

Textural properties of the supraparticles were analyzed using Hg intrusion measurements. The samples were degassed at 75 °C for 20 h, prior to each measurement. Mercury intrusion and

extrusion experiments were performed over a pressure range of 0.1 to 400 MPa by a PASCAL System (Thermo Scientific) using triple distilled mercury with a purity of >99.9995 %. The pore size distributions were calculated from the intrusion data using the Washburn equation with a contact angle of 141° and a surface tension of 480 mN m^{-1}.

Characterization of metal loadings

The Ga and Pt loadings of the prepared reference and SCALMS catalysts were determined by inductively coupled plasma atomic emission spectroscopy (ICP-AES) using a Ciros CCD (Spectro Analytical Instruments GmbH). The solid samples were digested with concentrated HCl:HNO_3:HF (attention: HF is a dangerous compound, relevant safety precautions must be taken) in a 3:1:1 volumetric ratio, using microwave heating to 493 K for 40 min. The instrument was calibrated for Pt (214.123 nm) and Ga (417.206 nm) with standard solutions of the elements before the analyses.

Catalytic testing – propane dehydrogenation in fixed bed reactor

To test the catalytic performance of the prepared catalysts in PDH, 1.5 g of each catalyst was loaded in a fixed bed quartz tubular reactor (Figure S2). The reactor was heated to the set point of 823 K and 0.12 MPa at 10 K min^{-1} under an inert atmosphere of 100 mL_N min^{-1} argon (99.998% purity, Air Liquide). Prior to the start of PDH, the catalyst was pretreated under the reductive atmosphere of 19.5 mL_N min^{-1} hydrogen (99.999% purity, Air Liquide) diluted with 80.5 mL_N min^{-1} argon for 3 h at 823 K. After the H_2 pretreatment, a purge stream of 100 mL_N min^{-1} of argon was sent for 60 minutes to remove any residual H_2. The reaction was started by supplying 8.9 mL_N min^{-1} propane (99.95% purity, Air Liquide) as feed gas diluted with 90.4 mL_N min^{-1} argon. The gas hourly space velocity (GHSV) was set at 3950 mL_{gas} $g_{Cat.bed}^{-1}$ h^{-1} under reaction conditions. The gases were dosed by mass flow controllers (MFC, Bronckhorst). All parts exposed to reagents, except for the fixed bed quartz reactor, were made of stainless-steel type 1.4571. A tubular split furnace heated the quartz glass fixed-bed reactor. All reactor tubes and pipes outside the furnace were held at 373 K by using heating tapes and fiberglass tape insolation.

Product analysis using online gas chromatography

The product gas mixture was analyzed using online gas chromatography (GC) on a Bruker 456 GC equipped with a GC-Gaspro column (30 m x 0.320 mm) having, a thermal conductivity detector (TCD) for detecting the light compounds (H_2, Ar, He) and a flame ionization detector

(FID) for detecting the C1-C3 hydrocarbons. The sample time for peak identification and resolving was 10 min. The peak area obtained from the GC data was used in calculating the mole fraction (x) of each compound. The conversion for propane ($X_{propane}$), the selectivity for the desired product propene ($S_{propene}$), deactivation rate ($Deactivation\ Rate\ K_d$) which describes the stability of the catalyst and the catalyst productivity ($Productivity$) were calculated using the equations below:

$$Conversion_{propane} = \frac{x_{propane,in} - x_{propane,out}}{x_{propane,in}} \quad (1)$$

$$Selectivity_{propene} = \frac{x_{propene}}{x_{propene} + x_{methane} + x_{ethane} + x_{ethene}} \quad (2)$$

$$Deactivation\ Rate\ K_d = \frac{\Delta X_{propane}}{\Delta TOS \cdot X_{1\ h\ TOS}} \quad (3)$$

$$Productivity = \frac{\dot{n}_{propane,in} . S_{propene} . X_{propane} . MW_{propene}}{m_{pt}} \quad (4)$$

Where x_i is the mole fraction of the respective compound i calculated based on the GC analysis, $\Delta X_{propane}$ and ΔTOS represents the net change in conversion and time between 1 h and 15 h time-on-stream (TOS) respectively. $\dot{n}_{propane,in}$ represents the mole flow rate of propane in the feed, $MW_{propene}$ is the molar weight of propene while m_{pt} represents the mass of Pt in the catalyst bed.

Ga nanoparticle yield determined from gallium sediment recycling experiments

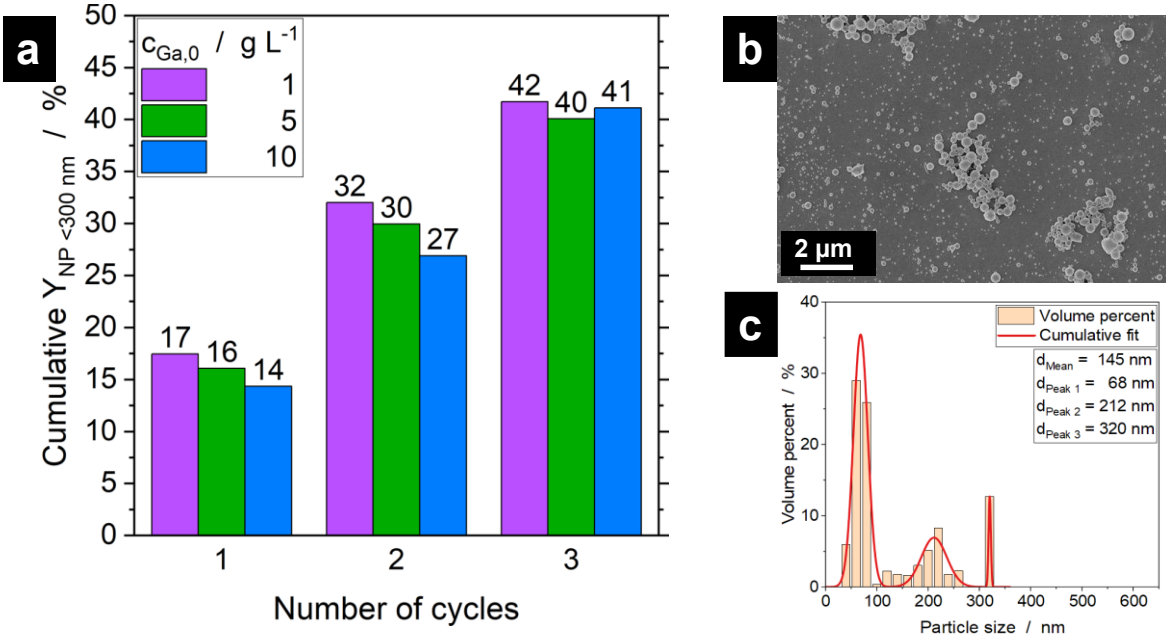

Figure S2. (a) Cumulative nanoparticles yield below 300 nm determined from gallium sediment recycling experiments over different gallium concentration $C_{Ga,0}$ = 1 – 10 g L^{-1}. (b) SEM image of Ga droplet dispersion after centrifugation at 1200 rpm for 10 min. Data obtained after 3rd cycle. (c) Volume-based distribution of Ga droplet dispersion centrifuged at 1200 rpm for 10 min. Data obtained after 3rd cycle. Process conditions: pre-melting of gallium, sonication time = 30 min, solvent = propan-2-ol (abs.), T_{max} = 35 °C, $C_{Ga,0}$ = 10 g L^{-1}, energy input = 1.04 J s^{-1}

Table S1. Metal loadings of all prepared GaPt SCALMS catalyst used in this study as determined by ICP-AES

Support pore size nm	Support type	GaPt droplet size distribution	Ga-loading wt%	Pt-loading wt%	Ga/Pt ratio -
0	silica	entire	5.33	0.33	45
10	silica	entire	4.20	0.24	49
10	silica	>300 nm	4.72	0.34	39
10	silica	<300 nm	6.68	0.41	46
45	supraparticles	<300 nm	7.91	0.45	50
100	supraparticles	<300 nm	5.48	0.34	45
200	supraparticles	<300 nm	5.35	0.36	42
320	supraparticles	<300 nm	5.97	0.35	48

Characterization of internal structure by cross-sectional TEM & nano-CT

The structure of and Ga and Pt particle distribution within SPs from the SP-45 nm and SP-320 nm samples were analyzed via transmission electron microscopy (TEM) using a Titan Themis^3 300 (FEI) transmission electron microscope and nano X-ray computed tomography (nano-CT) using a Zeiss Xradia 810 Ultra lab-based X-ray microscope. Additionally, Ga particles were dispersed onto a Lacey carbon supported copper TEM grid by dropcasting and were analyzed using a Titan Themis^3 300 (FEI) transmission electron microscope (with 15.7 mrad convergence half-angle, 91 mm camera length, 74 pA probe current, at sampling size of 2048 x 2048 pixel ,1.530 - 2.163 nm/pixel, and a dwell time of 5 µs. cf. Figure S6).

For cross-sectional TEM and nano-CT analysis, single particles (with SP-45 nm and SP-320 nm pore size each) were transferred to the tip of stainless-steel tomography needles. For this, the dry SP powder was first distributed on a glass plate and then, subsequently, a tomography needle covered with UV light-sensitive adhesive (UHU BOOSTER LED Light®; UH48150) was carefully brought into contact with one of the dispersed particles, so that a single SP with either 45 nm and 320 nm pore size stuck to the tip of the needle.

The nano-CT experiments were performed with a ZEISS Xradia 810 Ultra laboratory-scale X-ray microscope in high-resolution (HRES, field of view 16 µm x 16 µm, nominal optical resolution of 50 nm) phase contrast mode, equipped with a 5.4 keV rotating anode Cr source and a Zernike phase ring for phase contrast imaging. The 180° nano-CT tilt series of the SP (with 320 nm & 45 nm pore size) on the tomographic needles were acquired with an illumination time of 103-110 s/frame with 721 projections with 0.25° tilt increment. The tilt series were recorded in the native ZEISS microscope software (XMController and Scout&Scan). For the alignment of the tilt series, the Active Motion Compensation procedure[7] implemented in the natives ZEISS software (XMController) was utilized. The final 3D reconstruction was performed using a simultaneous iterative reconstruction technique (SIRT) algorithm[8] (100-150 iterations) implemented as an in-house Python script based on the Astra Toolbox.[9] Tilt series and reconstructions of all shown nano-CT experiments can be found in Video S1-4.

The cross-section lamellae for these two particle systems were extracted utilizing a FEI Helios NanoLab 660 Dual Beam SEM/FIB. A carbon protection layer of a few hundred nanometers was deposited in the dual-beam SEM/FIB with electron-induced deposition, prior to the ion-beam milling process. For the SP with a pore size of 320 nm (see Fig. S6), an extra ion-beam induced carbon layer was deposited to the free end of the lamella after trenching, to help support the lamella and avoid possible cracking during thinning. The final lamella, targeted at approximately 430 nm thickness, was finished with ion-beam showering at 2 keV beam energy. In this way, the ion-beam-induced sample damage was kept at a minimum level.

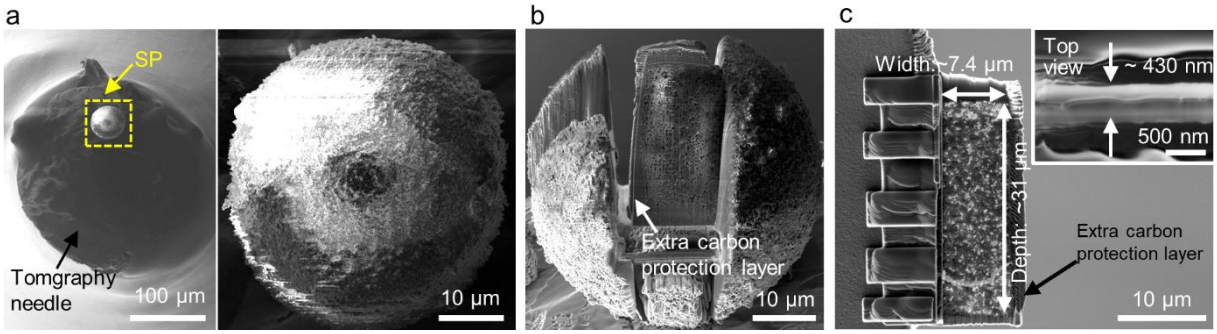

Figure S3. SEM images of the cross-section lamella preparation for the particle with 320 nm pore size. (a) SEM image of a single particle fixed on top of the tomography needle. (b) SEM image after trenching and deposition of an extra carbon protection layer to the free end of the lamella. (c) SEM image of the final lamella attached to the FIB grid.

The as-prepared lamellae were characterized with a Titan Themis^3 300 (FEI) operating at 300 kV. Elemental signals were analyzed using energy dispersive X-ray spectroscopy (EDXS). The data was acquired with the Thermo Fisher Sientific (TFS) Super-X detector and the STEM-EDXS maps and spectra were evaluated using TFS Velox software (3.12 version). For STEM-EDXS studies, we used a convergence half-angle of 15.7 mrad and a camera length of 91 mm. Furthermore, the following conditions were applied: probe current 117 pA, at sampling size (i.e., pixel size) of 3.060 nm/pixel, dwell time of 30 µs. The composition of the small particles distributed inside the SP was verified by STEM-EDXS, which reveals that they are completely composed of Pt. (Fig. S7a). Meanwhile, HAADF STEM images across the whole lamellae were acquired and stitched to get insight into the Pt NPs distribution inside the SPs (Fig. S7b and c). We counted the numbers of Pt NPs via adjusting the image contrast and then the Pt particle density, defined as the ratio of *(total number of Pt-NPs)/(analyzed lamella volume)*, was determined. It is revealed that the SPs with 320 nm pore size showed much higher Pt NPs

density (5.12/µm^3, 471 Pt NPs and the volume of lamella is 92.03 µm^3) than that of SPs with 45 nm pore size (2.35/µm^3, 91 Pt NPs and the volume of lamella is 38.78 µm^3).

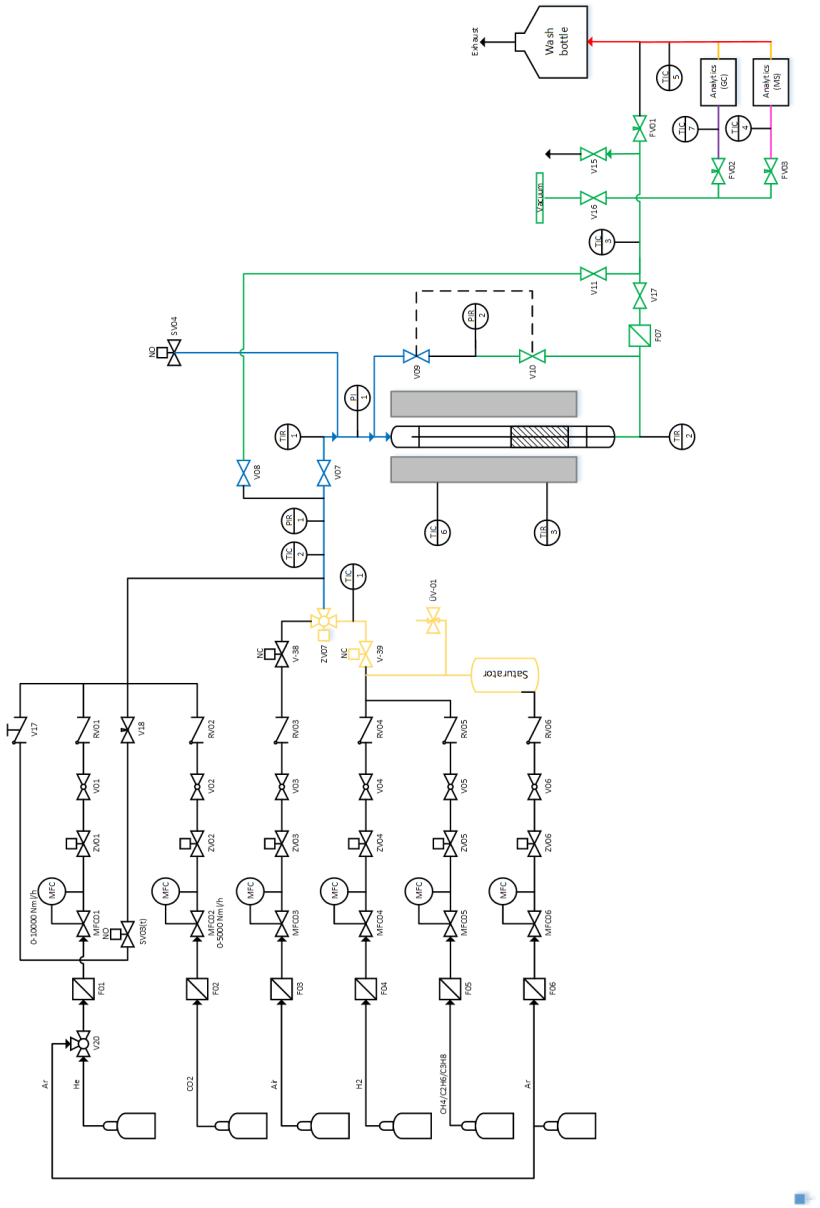

Figure S4: Flow scheme of the continuous gas-phase reactor used for propane dehydrogenation.

Characterization of Ga droplets before and after centrifugation

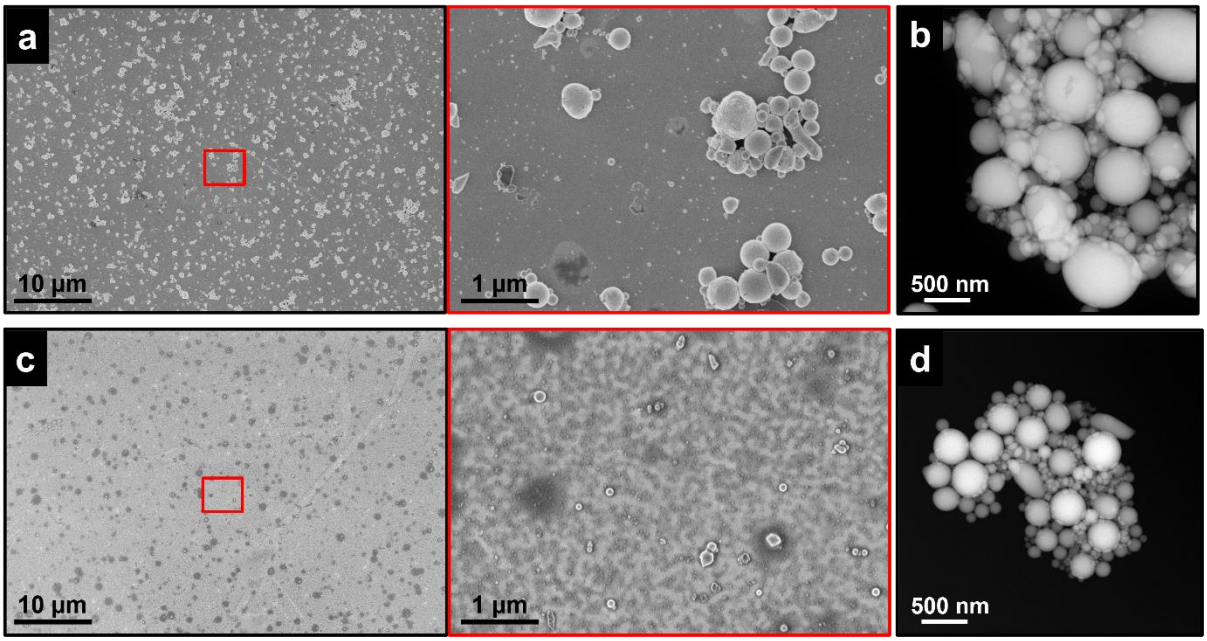

Figure S5. SEM and TEM analysis of Ga droplets. (a) SEM image and (b) HAADF-STEM image of the entire Ga droplet dispersion. (c) SEM image and (d) HAADF-STEM image of Ga droplet dispersion after centrifugation at 1200 rpm for 10 min. Process conditions: pre-melting of gallium, sonication time = 30 min, solvent = propan-2-ol (abs.), T_{max} = 35 °C, $C_{Ga,0}$ = 10 g L^{-1}, energy input = 1.04 J s^{-1}.

Characterization of supraparticles

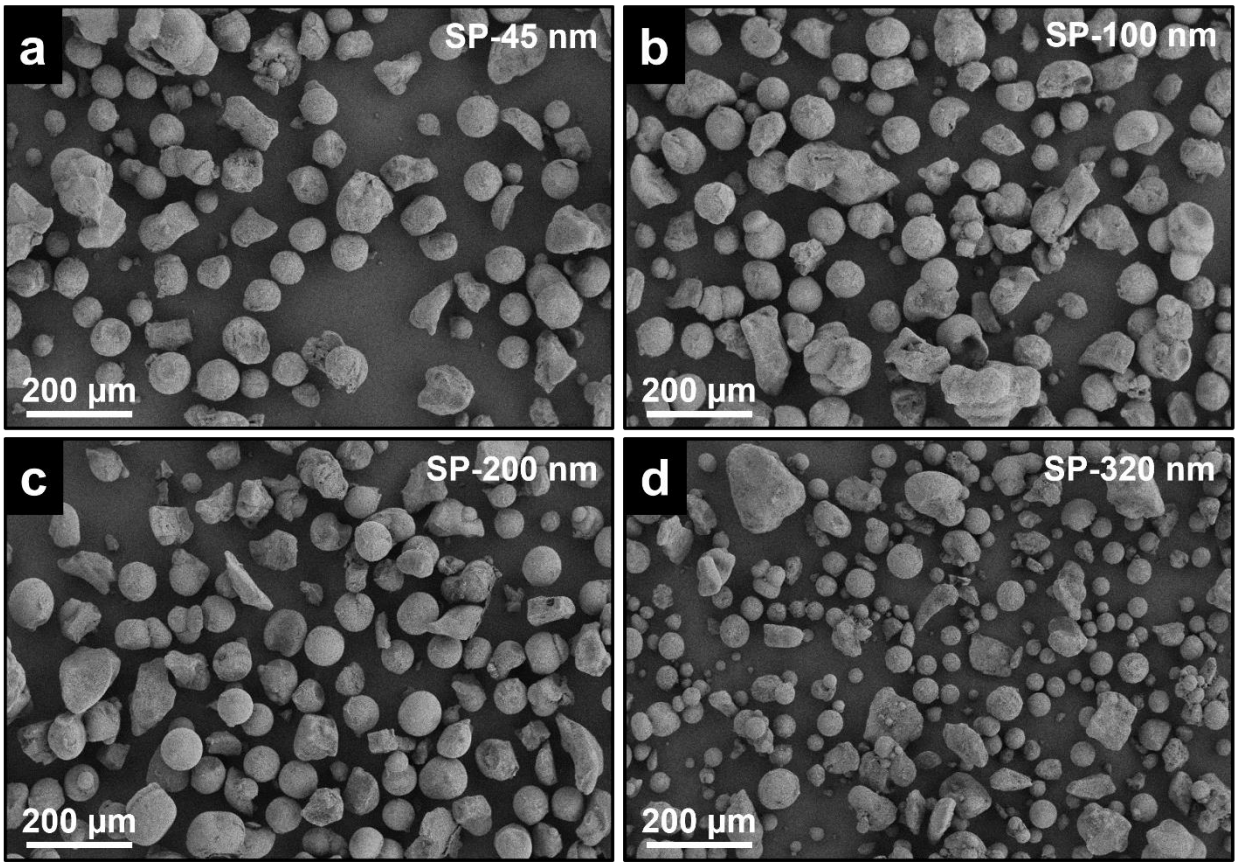

Figure S6. Supraparticle (SP) powder characterization. Low magnification SEM images of SP supports featuring average pore sizes of (a) 45 nm, (b) 100 nm, (c) 200 nm, (d) 320 nm.

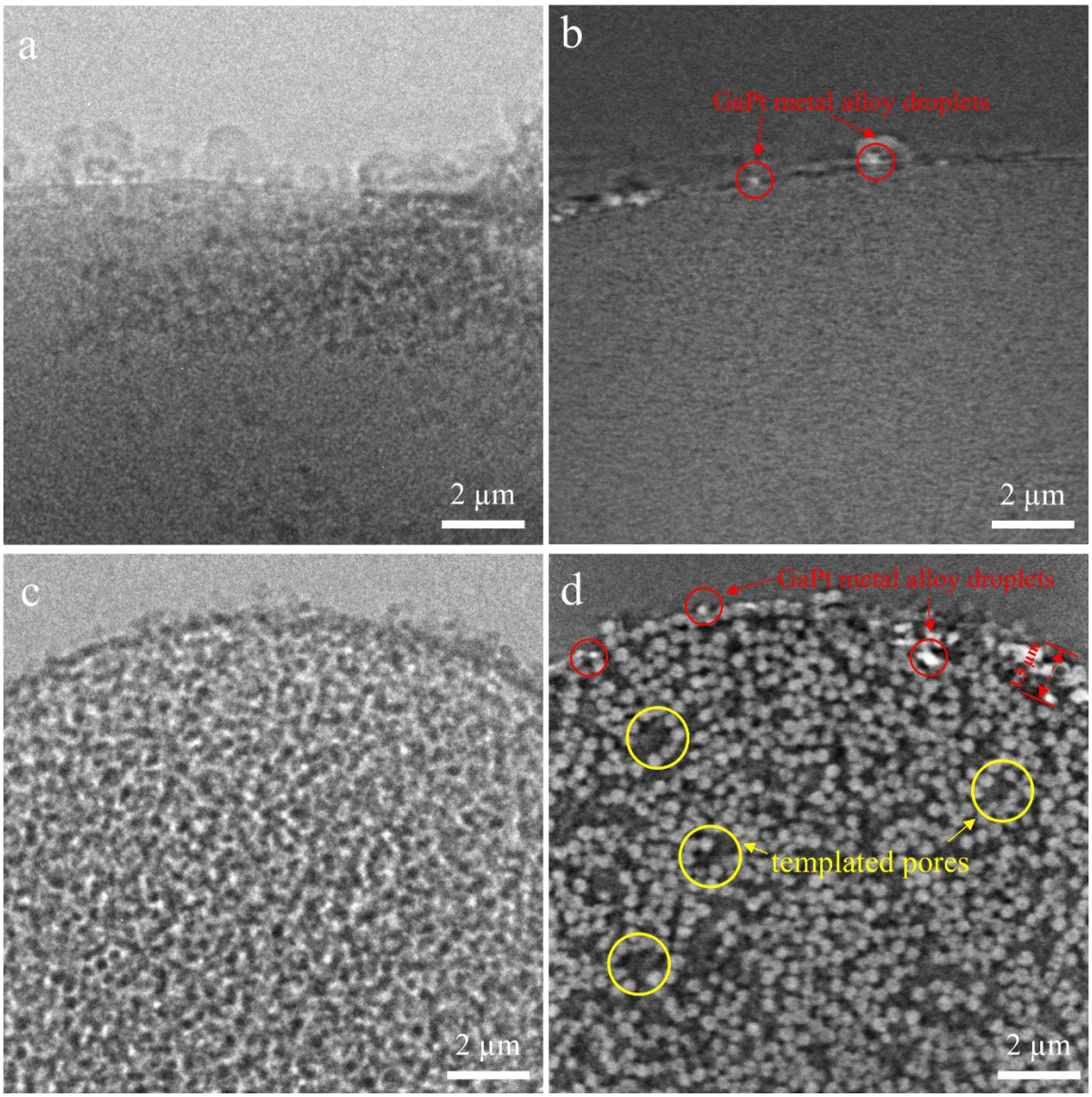

Figure S7. Tomography analysis of individual SP-based SCALMS Systems. (a, b) Single high-resolution nano-CT projections and single reconstructed slices of the SP-45 nm and (c,

d) of the SP-320 nm samples, which reveal that only the SP-320 nm sample exhibits a penetration of GaPt droplets into the outer rim of the porous template SP structure down to a depth of ~1.5 µm. However, deeper inside both SP samples, no larger GaPt droplets (> 50 nm, bright contrast in the reconstructed slices & dark in the projected images) are detected.

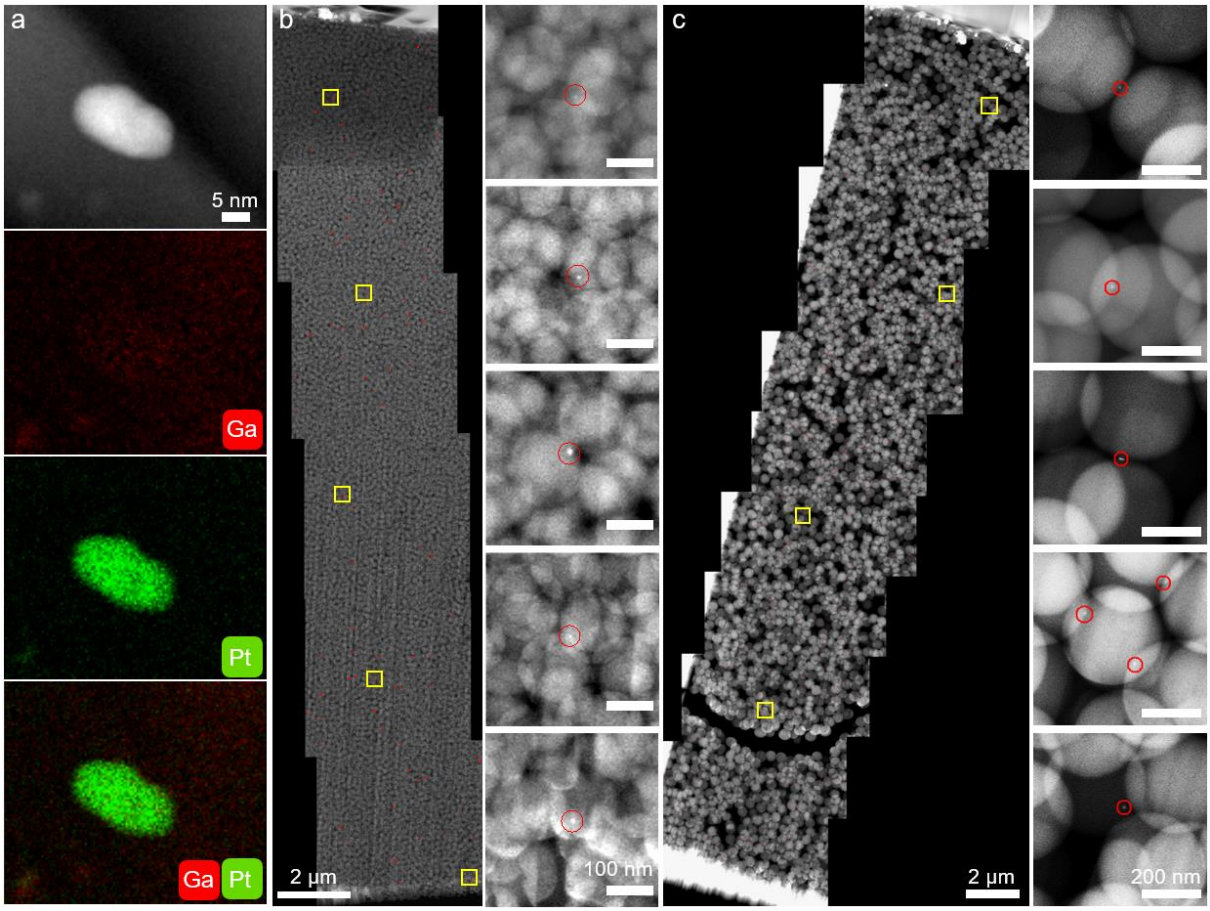

Figure. S8. Pt particle distribution and density within the SPs. (a) HAADF-STEM images and the corresponding EDXS maps verifying the particle is composed of Pt. (b and c) Stitched HAADF-STEM images and the zoomed-in images show the distribution of the Pt particles inside the SPs with pore size of 45 nm and 320 nm, respectively.

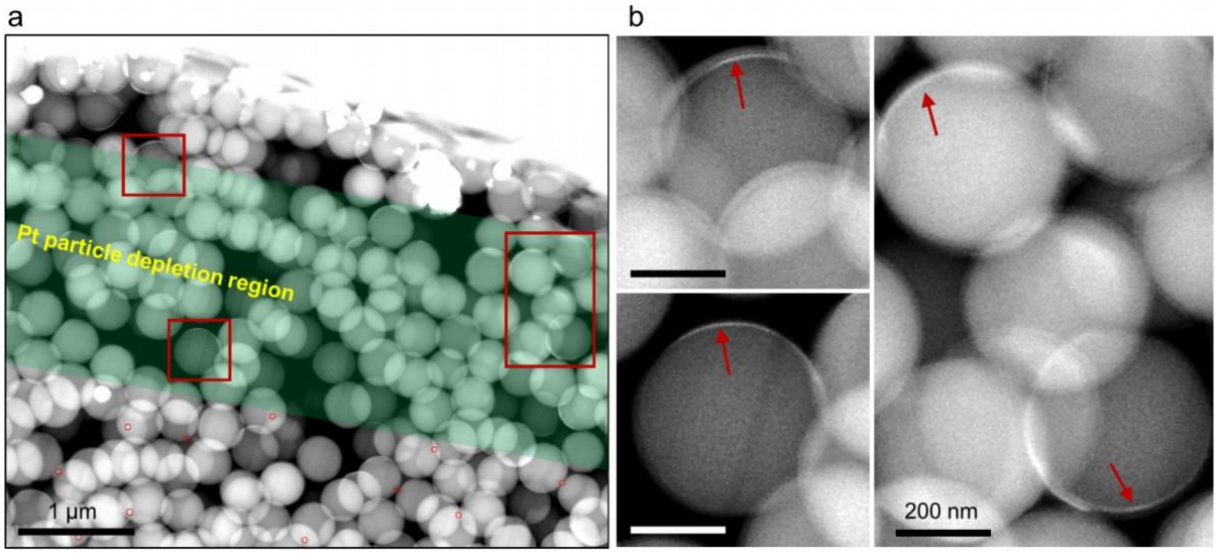

Figure. S9. (a) Pt-NP-depleted region close to the surface of SP-320 nm sample (highlighted in green) was distinguished via HAADF-STEM imaging. Pt NPs inside the SP are marked by red circles. (b) Zoomed-in images of the marked regions in (a) revealing the silica spheres were wetted by Ga. Red arrows indicate the periphery of the silica spheres wetted by Ga.

Propane dehydrogenation

Blank activity experiment: To confirm the absence of blank activity, the empty reactor and a bare SiO_2-10 nm support were tested under the same conditions of PDH.

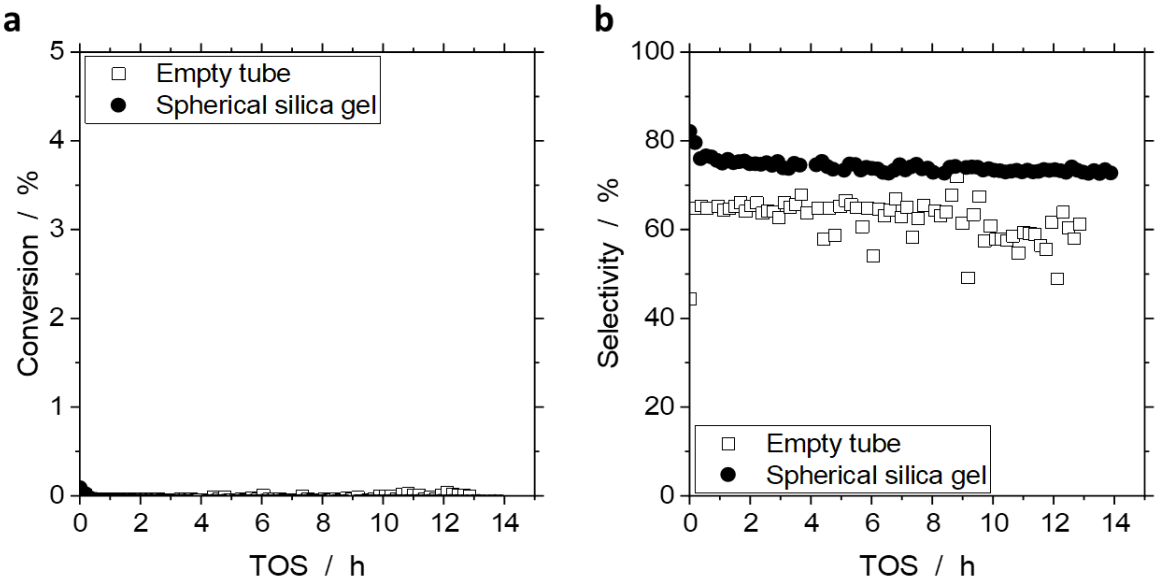

Figure S10. Conversion and selectivity for blank activity of empty reactor (open symbols) and bare SiO_2-10 nm support (filled symbol) in propane dehydrogenation. Catalyst bed: 1.5 g catalyst, H_2 pretreatment conditions: H_2 19.5 mL_N min^{-1}, Ar flow 80.5 mL_N min^{-1}, 823 K, 0.12 MPa, PDH reaction conditions: C_3H_8 flow 8.9 mL_N min^{-1}, Ar flow 90.4 mL_N min^{-1}, 823 K, 0.12 MPa, GHSV 3950 mL_{gas} $g_{Cat.bed}^{-1}$ h^{-1}.

Effect of GaPt droplet size on catalyst productivity: The catalyst productivity normalizes the activity of the catalyst per gram of the catalytically active metal, Pt.

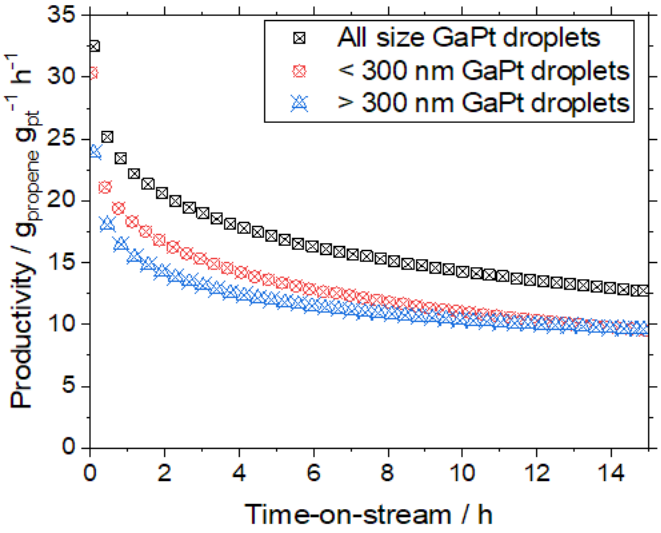

Figure S11. Catalytic performance of GaPt-SCALMS on commercial SiO_2 supports in propane dehydrogenation. a) Effect of GaPt droplet size on catalyst productivity. All size GaPt droplets (black), < 300 nm GaPt droplets (red), and > 300 nm GaPt droplets (blue). Catalyst bed: 1.5 g catalyst, H_2 pretreatment conditions: H_2 19.5 mL_N min^{-1}, Ar flow 80.5 mL_N min^{-1}, 823 K, 0.12 MPa, PDH reaction conditions: C_3H_8 flow 8.9 mL_N min^{-1}, Ar flow 90.4 mL_N min^{-1}, 823 K, 0.12 MPa, GHSV 3950 mL_{gas} $g_{Cat.bed}^{-1}$ h^{-1}.

Reference Experiment: To compare the activity of GaPt SCALMS with their monometallic counterpart, we tested the activity of Ga on SP-200 nm and Pt on SP-200 nm as references under the same conditions of PDH.

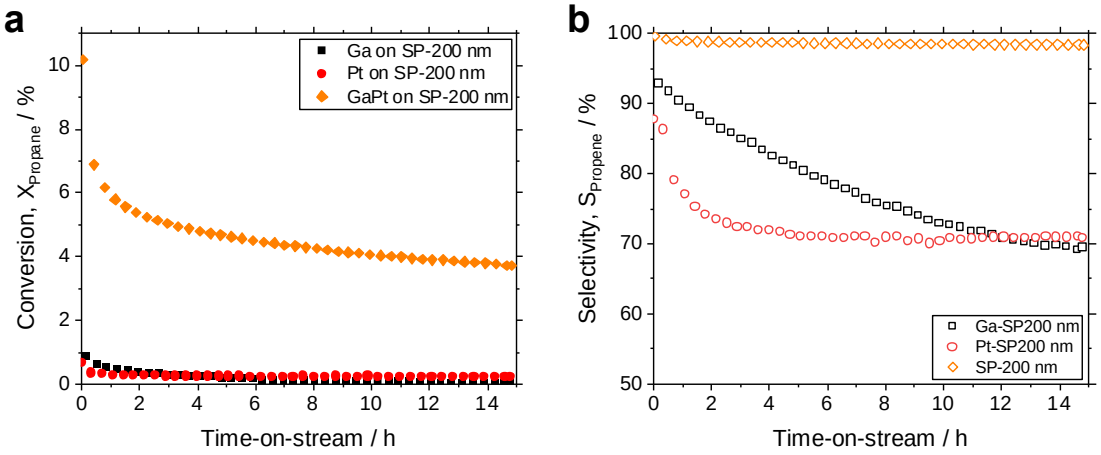

Figure S12. Conversion (filled symbol) and selectivity (open symbol) for reference experiments using Ga on SP-200 nm (black), Pt on SP-200 nm (red) and GaPt on SP-200 nm (orange) in propane dehydrogenation. Catalyst bed: 1.5 g catalyst, H_2 pretreatment conditions: H_2 19.5 mL_N min^{-1}, Ar flow 80.5 mL_N min^{-1}, 823 K, 0.12 MPa, PDH reaction conditions: C_3H_8 flow 8.9 mL_N min^{-1}, Ar flow 90.4 mL_N min^{-1}, 823 K, 0.12 MPa, GHSV 3950 mL_{gas} $g_{Cat.bed}^{-1}$ h^{-1}. Ga on SP-200 nm (Ga = 2.67 wt%), Pt on SP-200 nm (Pt = 0.34 wt%), GaPt on SP-200 nm (Ga = 5.35 wt%, Pt = 0.36 wt%).

Supplementary Videos

Video S1: Reconstructed slices of the nano-CT HRES PC tilt-series of < 300 nm GaPt droplets on SP-45 nm (MP4)

Video S2: Tilt series of the nano-CT HRES PC measurement of < 300 nm GaPt droplets on SP-45 nm (MP4)

Video S3: Reconstructed slices of the nano-CT HRES PC tilt-series of < 300 nm GaPt droplets on SP-320 nm (MP4)

Video S4: Tilt series of the nano-CT HRES PC measurement of < 300 nm GaPt droplets on SP-320 nm (MP4)

References

(1) Sudo, S.; Nagata, S.; Kokado, K.; Sada, K. Direct Synthesis of Liquid Metal Colloids and Their Transmetalation into Noble Metal Nanoparticles. *Chem. Lett.* **2014**, *43* (8), 1207–1209. DOI: 10.1246/cl.140359.

(2) Raman, N.; Wolf, M.; Heller, M.; Heene-Würl, N.; Taccardi, N.; Haumann, M.; Felfer, P.; Wasserscheid, P. GaPt Supported Catalytically Active Liquid Metal Solution Catalysis for Propane Dehydrogenation–Support Influence and Coking Studies. *ACS Catal.* **2021**, *11* (21), 13423–13433. DOI: 10.1021/acscatal.1c01924.

(3) Sebastian, O.; Al-Shaibani, A.; Taccardi, N.; Sultan, U.; Inayat, A.; Vogel, N.; Haumann, M.; Wasserscheid, P. Ga–Pt supported catalytically active liquid metal solutions (SCALMS) prepared by ultrasonication – influence of synthesis conditions on n-heptane dehydrogenation performance. *Catal. Sci. Technol.* **2023**, *13* (15), 4435–4450. DOI: 10.1039/D3CY00356F.

(4) Okamoto, H. Ga-Pt (Gallium-Platinum). *J. Phase Equilib. Diff.* **2007**, *28* (5), 494. DOI: 10.1007/s11669-007-9149-z.

(5) Bogush, G. H.; Tracy, M. A.; Zukoski, C. F. Preparation of monodisperse silica particles: Control of size and mass fraction. *J. Non-Cryst. Solids* **1988**, *104* (1), 95–106. DOI: 10.1016/0022-3093(88)90187-1.

(6) Vogel, N.; Viguerie, L.; Jonas, U.; Weiss, C. K.; Landfester, K. Wafer-Scale Fabrication of Ordered Binary Colloidal Monolayers with Adjustable Stoichiometries. *Adv. Funct. Mater.* **2011**, *21* (16), 3064–3073. DOI: 10.1002/adfm.201100414.

(7) Wang, J.; Karen Chen, Y.; Yuan, Q.; Tkachuk, A.; Erdonmez, C.; Hornberger, B.; Feser, M. Automated markerless full field hard x-ray microscopic tomography at sub-50 nm 3-

dimension spatial resolution. *Appl. Phys. Lett.* **2012**, *100* (14), 143107. DOI: 10.1063/1.3701579.

(8) Gilbert, P. Iterative methods for the three-dimensional reconstruction of an object from projections. *J. Theor. Biol.* **1972**, *36* (1), 105–117. DOI: 10.1016/0022-5193(72)90180-4.

(9) van Aarle, W.; Palenstijn, W. J.; Beenhouwer, J. de; Altantzis, T.; Bals, S.; Batenburg, K. J.; Sijbers, J. The ASTRA Toolbox: A platform for advanced algorithm development in electron tomography. *Ultramicroscopy* **2015**, *157*, 35–47. DOI: 10.1016/j.ultramic.2015.05.002.